NKCC2 Surface Expression in Mammalian Cells

Boubacar Benziane, Sylvie Demaretz, Nadia Defontaine, Nancy Zaarour, Lydie L Cheval, Soline Bourgeois, Christophe Klein, Marc Froissart, Anne Blanchard, Michel Paillard, et al.

THE JOURNAL OF BIOLOGICAL CHEMISTRY VOL. 282, NO. 46, pp. 33817–33830, November 16, 2007

NKCC2 Surface Expression in Mammalian Cells

*DOWN-REGULATION BY NOVEL INTERACTION WITH ALDOLASE B**

Received for publication, January 8, 2007, and in revised form, August 17, 2007 Published, JBC Papers in Press, September 11, 2007, DOI 10.1074/jbc.M700195200

Boubacar Benziane[‡§], Sylvie Demaretz[‡§], Nadia Defontaine[‡§], Nancy Zaarour[‡§], Lydie Cheval[§¶], Soline Bourgeois[‡§], Christophe Klein[§], Marc Froissart[‡§‖], Anne Blanchard[‡§‖], Michel Paillard[‡§‖], Gerardo Gamba[**], Pascal Houillier[‡§‖], and Kamel Laghmani[‡§1]

From [‡]INSERM U652, 75006 Paris, France, [¶]CNRS-UPMC UMR7134, 75006 Paris, France, [§]IFR58, Institut des Cordeliers, 75006 Paris, France, Universite Paris-Descartes, 75006 Paris, France, [**]Instituto Nacional de Ciencias Medicas y Nutricion Salvador Zubiran and Instituto de Investigaciones Biomedicas, Universidad Nacional Autonoma de Mexico, Tlalpan, Mexico City 14000, Mexico, and [‖]AP-HP, Departement de Physiologie, Hopital Europeen Georges Pompidou, 75015 Paris, France

Apical bumetanide-sensitive Na^+-K^+-$2Cl^-$ co-transporter, termed NKCC2, is the major salt transport pathway in kidney thick ascending limb. NKCC2 surface expression is subject to regulation by intracellular protein trafficking. However, the protein partners involved in the intracellular trafficking of NKCC2 remain unknown. Moreover, studies aimed at understanding the post-translational regulation of NKCC2 have been hampered by the difficulty to express NKCC2 protein in mammalian cells. Here we were able to express NKCC2 protein in renal epithelial cells by tagging its N-terminal domain. To gain insights into the regulation of NKCC2 trafficking, we screened for interaction partners of NKCC2 with the yeast two-hybrid system, using the C-terminal tail of NKCC2 as bait. Aldolase B was identified as a dominant and novel interacting protein. Real time PCR on renal microdissected tubules demonstrated the expression of aldolase B in the thick ascending limb. Co-immunoprecipitation and co-immunolocalization experiments confirmed NKCC2-aldolase interaction in renal cells. Biotinylation assays showed that aldolase co-expression reduces NKCC2 surface expression. In the presence of aldolase substrate, fructose 1,6-bisphosphate, aldolase binding was disrupted, and aldolase co-expression had no further effect on the cell surface level of NKCC2. Finally, functional studies demonstrated that aldolase-induced down-regulation of NKCC2 at the plasma membrane was associated with a decrease in its transport activity. In summary, we identified aldolase B as a novel NKCC2 binding partner that plays a key role in the modulation of NKCC2 surface expression, thereby revealing a new regulatory mechanism governing the co-transporter intracellular trafficking. Furthermore, NKCC2 protein expression in mammalian cells and its regulation by protein-protein interactions, described here, may open new and important avenues in studying the cell biology and post-transcriptional regulation of the co-transporter.

Cation-Cl co-transporters (CCCs)[2] mediate the coupled movement of sodium and/or potassium to that of chloride across the plasmalemma of animal cell (1). In polarized tissues, cation-Cl co-transport is involved in net transepithelial salt movement. They can be divided into sodium-dependent transporters, such as Na-K-2Cl co-transporters and the NaCl co-transporter and Na^+-independent KCl co-transporters. All of the CCCs exhibit similar hydropathy profiles with 12 transmembrane spanning domains, an N terminus of variable length, and a long cytoplasmic C terminus (2). Two isoforms of the Na-K-2Cl co-transporter (NKCC) protein are currently known (3). NKCC1, the basolateral isoform, is by far the most widely distributed (4, 5). By contrast, NKCC2 is exclusively targeted to the apical cell surface and is exclusively found in the kidney (4, 6). Apical sodium entry in the thick ascending limb of the loop of Henle is mediated by NKCC2. Mutations of NKCC2 have been linked to some forms of Bartter syndrome, a severe human genetic disease involving NaCl wasting and hypokalemic alkalosis with hypercalciuria (7, 8). Immunolocalization experiments revealed that NKCC2 is expressed not only at the cell surface but also in a population of subapical vesicles raising the hypothesis that intracellular trafficking may regulate NKCC2 membrane expression (9). In agreement with this hypothesis, vasopressin (AVP) induces the shuttling of these vesicles to the cell membrane leading to an increase in apical NKCC2 protein expression and activity (10). Likewise, recent reports showed that cAMP increases surface expression of NKCC2 in rat thick ascending limbs (11). Intracellular regulation of protein trafficking generally involves protein-protein interactions. Such mechanisms have been reported for the basolateral isoform, NKCC1. Proteins that bind to NKCC1 include SPAK and OSR1, PP1, PP2A, CIP, and Hsp90 (12–17). The identification of several NKCC1-binding proteins supported further the view that regulation of NKCC2 might also involve a network of protein-protein interactions. In contrast to NKCC1, little is known about the protein partners of NKCC2. More specifically, the

* This work was supported by grants from INSERM, Paris, France. The costs of publication of this article were defrayed in part by the payment of page charges. This article must therefore be hereby marked "*advertisement*" in accordance with 18 U.S.C. Section 1734 solely to indicate this fact.

[1] To whom correspondence should be addressed: INSERM U652, 15 Rue de l'Ecole de Medecine, 75270 Paris Cedex 06, France. Tel.: 33-1-44-41-37-10; Fax: 33-1-44-41-37-17; E-mail: Kamel.Laghmani@bhdc.jussieu.fr.

[2] The abbreviations used are: CCC, cation-Cl co-transporter; TAL, thick ascending limb; MKTAL, mouse kidney thick ascending limb; MTAL, medullary TAL; RT, reverse transcription; FBP, fructose 1,6-bisphosphate; HA, hemagglutinin; PBS, phosphate-buffered saline; GFP, green fluorescent protein; OKP, opossum kidney cells; MCS, multiple cloning site; AA, amino acid; NKCC, Na-K-2Cl co-transporter; AVP, arginine vasopressin.

protein partners involved in the intracellular trafficking of NKCC2 remain unknown. Furthermore, previous attempts failed to express NKCC2 proteins in mammalian cells, and as a consequence, little is known about the post-translational regulations of the co-transporter. In this study, we report that we were able to address this issue by N-terminally tagging NKCC2 protein. In addition, to identify potential interacting partners of NKCC2, we screened a kidney cDNA expression library by the yeast two-hybrid assay using NKCC2 C terminus as bait. Among the positive identified clones, several matched the sequence of aldolase B. Aldolase B is a glycolytic enzyme that has specialized functions in fructose metabolism and gluconeogenesis (18, 19). However, several studies reported that besides its principal role in the carbohydrate metabolism, aldolase could also exert other functions in the cell (20–27). In this study, we demonstrate that the proximal C-terminal domain of NKCC2 can specifically associate with aldolase B and that this interaction might play a crucial role in the control of apical NKCC2 expression in the kidney.

EXPERIMENTAL PROCEDURES

Materials

All chemicals were obtained from Sigma unless otherwise noted. Penicillin and streptomycin were from Invitrogen.

Subclonings were carried out with the following vectors: 1) pGKT7 (Clontech), which contains the binding domain DNA of GAL4, a multiple cloning site (MCS), and a kanamycin resistance gene ($KANA^r$); 2) pCMV-Myc (Clontech), which contains epitope c-Myc, an MCS, and an ampicillin resistance gene (AMP^r); 3) pcDNA3.1/V5-His-TOPO (Invitrogen), which contains epitope V5, an MCS, and an AMP^r resistance gene; 4) pEGFP-C2 (Clontech) which contains green fluorescent protein (GFP) gene, an MCS, and a $KANA^r$ resistance gene.

Cell Culture

Mouse kidney thick ascending limb (MKTAL) cells (28) were grown on plastic culture dishes in Dulbecco's modified Eagle's medium/NUT F-12 medium (Invitrogen) containing 5% fetal calf serum (Biowest), penicillin (50 IU/ml), and streptomycin (5 μg/ml) (Invitrogen). OKP (a clonal of opossum kidney cell line) cells, kindly provided by Prof. R. Alpern (Department of Internal Medicine, University of Texas Southwestern Medical Center, Dallas) were passaged in high glucose (450 mg/dl) Dulbecco's modified Eagle's medium supplemented with 10% fetal bovine serum (Invitrogen), penicillin (100 units/ml), and streptomycin (100 μg/ml). For DNA transfection, cells were grown to 60–70% confluence and then were transiently transfected for 6 h with plasmids using the Lipofectamine plus kit according to the manufacturer's instructions (Invitrogen) and grown to 100% confluence. Cells for control and experimental groups are always derived from the same flask and passage and were studied on the same day.

Immunoprecipitation

Cells were solubilized with lysis buffer (0.4 M NaCl; 0.5 mM EGTA; 1.5 mM $MgCl_2$;10 mM Hepes, pH 7.9; 5% (v/v) glycerol; 0.5% (v/v) Nonidet P-40) and protease inhibitors (Complete, Roche Diagnostics). Immunoprecipitation was carried out using the antibody of interest followed by affinity purification using protein G-agarose beads (Dynal). The antibodies used in this study were the following: mouse anti-Myc and anti-HA antibodies (Clontech), mouse anti-V5 antibody (Invitrogen), and goat anti-aldolase antibody (Euromedex). After incubation with protein G-agarose beads for 1 h at room temperature, the immunocomplex was washed three times in PBS (Invitrogen). The protein samples were boiled in loading buffer, run on gradient 6–20% SDS-polyacrylamide gels, probed with primary antibodies of interest and horseradish peroxidase-conjugated secondary antibody, according to standard procedures. Proteins were visualized by enhanced chemiluminescence detection (PerkinElmer Life Sciences) following the manufacturer's instructions.

Immunocytochemistry

Cultures to be immunostained were washed with PBS and fixed with 2% paraformaldehyde in PBS for 20 min at room temperature, incubated for 5 min with 50 mM NH_4Cl, permeabilized with 0.1% Triton X-100 for 1 min, and incubated with DAKO (antibody diluent with background-reducing components; DAKO, Carpinteria) for 30 min to block nonspecific antibody binding. Indirect immunofluorescence was carried out using the antibodies of interest. Cells were incubated for 1 h at room temperature or overnight at 4 °C with primary antibodies diluted in DAKO. Treatment with the anti-V5 antibody was followed by the addition of a Texas Red-conjugated secondary antibody (Jackson ImmunoResearch). Anti-aldolase and anti-Myc antibodies were visualized with a biotinylated anti-goat IgG antibody and Cy3-labeled streptavidin (*red*) and Cy2-labeled anti-mouse (*green*) IgG antibodies, respectively. Cells were then washed with PBS and mounted with Vectashield (Vector Laboratories).

Biotinylation

Cells were transfected with a full-length NKCC2 tagged with Myc and/or aldolase B tagged with V5. After 48 h cells were placed on ice and rinsed twice with a cold rinsing solution containing PBS, pH 7.5, 1 mM $MgCl_2$, and 0.1 mM $CaCl_2$. Cells were then gently agitated at 4 °C for 1 h in borate buffer, pH 9, containing 1 mg/ml NHS-biotin. They were rinsed three times in quenching solution (rinsing solution with 100 mM glycine added) and agitated at 4 °C in quenching solution for 20 min. Then they were washed three times in PBS, pH 7.5, 1 mM $MgCl_2$, and 0.1 mM $CaCl_2$, and cells were lysed for 45 min at 4 °C in solubilizing buffer (150 mM NaCl, 5 mM EDTA, 3 mM KCl,120 mM Tris/Hepes, pH 7.4; 1% (v/v) Triton X-100) containing protease inhibitors (Complete 1697498, Roche Diagnostics). Samples were harvested, sonicated, and centrifuged at 16,000 rpm for 15 min at 4 °C.

Aliquots of the lysate were normalized to 1 mg/ml, and aliquots were taken for total lysate fraction, and the rest of aliquots were incubated in avidin beads (Sigma) overnight at 4 °C. After overnight incubation, samples were centrifuged at 16,000 rpm for 5 min, and the supernatant (the intracellular fraction) was removed. Avidin beads were then washed with solubilizing buffer and then centrifuged for 7 min at 16,000 rpm seven

times. Pellets were incubated in solubilizing buffer and denaturating buffer for 10 min at 95 °C and stored at −20 °C. Each fraction was subjected to SDS-PAGE and Western blot analysis.

Site-directed Mutagenesis

The QuikChange site-directed mutagenesis method (Stratagene) was used to mutate the two predicted glycosylations sites, Asn-442 and Asn-452 to glutamine, using the custom-made (MWG Biotec) oligonucleotides 5′-gatgccactggcagcatgcaagacaccatcgtttc-3′ and 5′-atgaattgccaaggctctgcggcctg-3′, respectively. The latter primer was used to create double mutants (N442Q,N452Q). All mutations were confirmed by automated sequencing.

Yeast Two-hybrid Screening

Construction of the GAL4 BD:Bait Gene Fusion—The cDNA fragment containing the first 108 AA of NKCC2 C-terminal tail region (named NKCC2 C1-term) was amplified by high fidelity PCR using the following primers: 5′-ccggaattcgacaacgctctggaattaac-3′ (sense) and 5′-cgcgtcgaccattctccccaagcctga-3′ (reverse). After restriction enzyme digestion with EcoRI and SalI, the cDNA fragment was cloned into pGBKT7 vector carrying the TRP1 selection marker. DNA sequencing confirmed that the cDNA encoding the C-terminal domain of NKCC2 (bait) was in-frame with GAL4 BD.

Testing the BD-NKCC2-C1-terminal Plasmid for Transcriptional Activation—To check for autoactivation of reporter gene promoters, the yeast reporter strain AH109 was transformed with the BD-NKCC2C1-terminal plasmid. The AH109 reporter contains three reporter genes, *ADE2*, *HIS3*, and *lacZ*, under the control of distinct upstream activating sequences and TATA boxes. These promoters yield strong and specific interaction to GAL4. Yeast cells were grown in YPDA medium (Clontech) complemented with 0.003% adenine hemisulfate. For transformation, a YPDA culture from AH109 (50 ml) grown to an A_{600} of ~1 (18 h) was centrifuged at 1200 × *g* for 3 min, washed with 50 ml of distilled H_2O, and resuspended in 1 ml of distilled H_2O. Aliquots of 50 μl were treated with 240 μl of polyethylene glycol (50% w/v), 36 μl of 1 M LiAc, 25 μl of single-stranded DNA (2.0 mg/ml), 50 μl of distilled H_2O, and 1 μg of plasmid. Transformed cells were plated on synthetic complete medium lacking the amino acids tryptophan, histidine, and/or adenine. The results indicated that the BD-NKCC2-C1-terminal construct did not autoactivate the reporter genes because no growth was observed.

Library Screening—The GAL4 AD:cDNA library constructed in the yeast plasmid pACT2 from human kidney was purchased from Clontech. The cDNA library was already pretransformed into *Saccharomyces cerevisiae* host strain Y187. The cDNA library plasmid pACT2 contains the ampicillin gene for selection in *Escherichia coli* and a leucine marker for selection in the yeast host. Pretransformed libraries are screened by mating. AH109 transformed with NKCC2-C1term-BD plasmid was inoculated into 50 ml of SD lacking Trp and incubated at 30 °C overnight (18 h) with shaking at 250–270 rpm. After growing to an A_{600} of ~1.5, the yeast culture was centrifuged at 1000 × *g* for 5 min. The pellet was resuspended in the residual liquid (~5 ml) by vortexing. For mating, the entire AH109 culture was combined with a 1-ml aliquot of the pretransformed library culture in a 2-liter sterile flask. After adding 45 ml of 2× YPDA/kanamycin medium, cells were incubated at 30 °C overnight with gentle swirling (30–50 rpm). After 20 h of mating, cells were centrifuged at 1000 × *g* for 10 min. The pellet was resuspended in 10 ml of 0.5× YPDA/kanamycin medium, plated selection medium lacking histidine, leucine, and tryptophan, and incubated at 30 °C. The plates were checked for colonies after 4 days of incubation at 30 °C, and positive colonies were transferred to high stringency selection medium plates lacking *Ade*, *His*, *Leu*, and *Trp* and incubated at 30 °C for 2–3 days. Ade^+, His^+, Leu^+, Trp^+ transformant colonies were then rescreened by colony-lift assay for LacZ activity, and colonies that activated all of the reporter genes in the AH109 stain were further analyzed.

Isolation and Sequence Analyses of Positive AD:cDNA Clones—AD:cDNA plasmids encoding the putative interacting proteins were isolated from yeast cells using an RPM yeast plasmid isolation kit (Bio 101, Inc., Vista, CA). Prey plasmids were rescued by transformation into DH5α bacteria (Invitrogen) and isolated using a kit from Qiagen. Insert sizes were checked by BglII digestion. cDNA plasmids were then sequenced and assessed using the BLAST program.

Animals

Experiments were carried out on male C57BL/6J mice (8–10 week old; Charles Rivers Breeding Laboratories). Mice had free access to food (semi-synthetic diet; SAFE, Epinay, France) and were allowed to drink water *ad libitum*.

Isolation of Medullary and Cortical Thick Ascending Limb

After pentobarbital anesthesia (140 mg/g body weight, intraperitoneally), the left kidney was quickly perfused through the abdominal aorta with 5 ml of Hanks' modified microdissection solution and then with the same solution supplemented with 0.25% (w/v) collagenase (Serva, Heidelberg, Germany). The kidney was sliced along the cortico-papillary axis in small pieces, which were incubated for 10 min at 30 °C in collagenase-containing (0.15% (w/v) microdissection solution. After rinsing, medullary and cortical thick ascending limbs were dissected at 4 °C under stereomicroscopic observation and were identified by morphological and topographical criteria as described previously (29).

Total RNA Extraction, Reverse Transcription, Conventional RT-PCR, and Real Time PCR Analysis

Total RNAs were extracted from pools of nephron segments (2–3 cm length) by using a microadaptation of the method of Chomczynski and Sacchi, and reverse-transcribed using the First-Strand cDNA synthesis kit for RT-PCR (Roche Diagnostics), according to the manufacturer's protocol using random hexamers. Real time PCR was performed on a LightCycler (Roche Diagnostics) with the DyNAmo™ CapillarySYBR Green quantitative PCR kit (Ozyme) according to the manufacturer's protocol, except that the final reaction volume was reduced to 8 ml. Each reaction was performed on the equivalent of 0.25 mm of microdissected MTAL. Primers used were chosen from the published mouse aldolase B, NKCC2, and car-

bonic anhydrase XIV cDNA sequences and were designed using LightCycler Probe Design (Roche Diagnostics) software. The sequences of the used primers were 5′-ctgaaattgcccagcg-3′ (sense) and 5′-agagggtctcgtggaa-3′ (reverse) for aldolase B, 5′-gagattggcgtggtcatagtcagaa-3′ (sense) and 5′-tgctgctgatgtt-gccgtcttt-3′ (reverse) for NKCC2, and 5′-gaagggacatacg-gagagggcag-3′ (sense) and 5′-gaagggacatacggagagggcag-3′ (reverse) for carbonic anhydrase XIV. Samples were submitted to 45 cycles of three temperatures steps as follows: 95 °C for 10 s, 60 °C for 20 s, and 72 °C for 13 s. In the experiment, a standardization curve was made using serial dilutions (1 to 1:500) of a cDNA stock solution from total kidney.

Total RNA extraction from MTAL and MKTAL cells was carried out with the RNeasy midi kit (Qiagen, Hilden, Germany) according to the manufacturer's instructions. cDNA was synthesized from total RNA using Superscript II RT with random primers incubated at 25 °C for 10 min and at 42 °C for 50 min. The reaction was stopped by incubation at 75 °C for 15 min. A negative RT-PCR was performed with H_2O as a replacement of superscript II. For PCR, 2 μl of the cDNA solution was supplemented with 5 μl of 10× PCR buffer, 1 μl of 50 mM $MgCl_2$, 10 pmol of each primer, 1 μl of a 10 mM dNTP solution, and 1.25 units of *Taq* polymerase in a final volume of 50 μl. The sequence of the used primers to amplify full-length mouse aldolase B and NKCC2 cDNAs were 5′-gaggactcttccccttttgct-3′ (sense) and 5′-ataggtgtaggaggctgtga-3′ (reverse) for aldolase, and 5′-atgtcggtcagcatcccttcc-3′ (sense) and 5′-ttaagagtaaaatgt-taagac-3′ (reverse) for NKCC2 (30). Samples were denatured at 95 °C for 4 min, followed by 35 cycles of 95 °C for 1 min, 58 °C for 1 min, and 72 °C for 1.5 min. Final extension was for 10 min at 72 °C. The PCR products were size fractionated on 1–2% agarose gels stained with ethidium bromide.

Measurement of Intracellular pH and Na-K-2Cl Co-transporter Activity

Measurement of cytoplasmic pH (pH_i) was accomplished in cells grown to confluence on coverslips using the intracellularly trapped pH-sensitive dye 2′,7′-bis(carboxyethyl)-5,6-carboxy-fluorescein. pH_i was estimated from the ratio of fluorescence with excitation wavelengths of 495 and 450 nm and emission wavelength 530 nm (Horiba Jobin Yvon, France). Calibration of the 2′,7′-bis(carboxyethyl)-5,6-carboxyfluorescein excitation ratio was accomplished using the nigericin technique. Na-K-2Cl co-transport activity was measured as bumetanide-sensitive NH_4 influx, as described previously (31, 32). Cells were first bathed at 37 °C in a CO_2-free Hepes/Tris-buffered medium containing (in mM) 135 NaCl, 10 Hepes (pH 7.4), 5 KCl, 1 $MgCl_2$, 0.8 KH_2PO_4, 0.2 K_2HOP_4, 1 $CaCl_2$, and 10 $BaCl_2$, to measure base-line pH_i. 20 mM NH_4Cl was then added to the medium (isosmotically replacing NaCl). After NH_4Cl addition, a very rapid initial cellular alkalinization (ΔpH_i) occurred because of immediate NH_3 entry, which stopped when intracellular, and extracellular [NH_3] became equal (NH_3 equilibrium). The initial alkalinization was then followed by a pH_i recovery (dpH_i/dt). The ΔpH_i caused by NH_4Cl addition was used to calculate the cell buffer capacity (βi) as described previously (33). Transfecting OKP cells with myc-NKCC2 in the presence or the absence of aldolase-V5 had no effect neither on base-line pH_i nor on the magnitude of the initial alkalinization when compared with mock-transfected cells. Consequently, βi was not different between the three groups. The mean values of βi (H^+/liter/pH unit) were 29.32 ± 2.7 ($n = 3$) in mock-transfected cells, 31.11 ± 2.5 ($n = 5$) in OKP cells expressing myc-NKCC2, and 32.33 ± 2.4 ($n = 5$) in cells co-transfected with myc-NKCC2 and aldolase-V5 constructs. Therefore, Na-K-2Cl co-transporter activity is expressed as dpH_i/dt.

Statistics

Results are expressed as mean ± S.E. Differences between means were evaluated using paired or unpaired *t* test or analysis of variance as appropriate. $p < 0.05$ was considered statistically significant.

RESULTS

NKCC2 Expression in Mammalian Cells—To date, no one has been able to express NKCC2 protein in mammalian cells. Indeed, several attempts failed to stably express the co-transporter in transfected mammalian cells such as COS (SV40-transformed simian cell line), HEK293 (human embryonic kidney), NIH 3T3 (mouse NIH/Swiss embryo fibroblast line), and Madin-Darby canine kidney cells (34–36). Interestingly, it has been shown previously that position- and sequence-specific tagging is crucial to generate a stable protein expression in cell culture (37, 38). Most importantly, it has been reported that the degradation of several proteins can be blocked following fusion of the Myc tag to their N terminus (37–40). Hence, we anticipated that we could successfully express NKCC2 protein by tagging its N-terminal domain with Myc. Therefore, full-length mouse NKCC2 cDNA was cloned into pCMV-expression vector downstream of the c-Myc tag and used for transient transfection in either OKP or MKTAL cells, two models of previously characterized renal epithelial cell lines (28, 41, 42). The expression of NKCC2 protein was determined by Western blot following immunoprecipitation using anti-Myc antibody. As illustrated in Fig. 1*A*, Myc-NKCC2 protein in cell lysates of OKP and MKTAL cells was detected as two bands, one around 160 kDa and the other around 120 kDa. As negative controls, these bands were not detected neither in mock-transfected cells nor when immunoprecipitation was carried out using anti-V5 or anti-HA antibodies indicating that the observed signal is specific to Myc-NKCC2 fusion protein. Cells treatment with peptide:*N*-glycosidase and endoglycosidase H (data not shown) revealed that these bands correspond to the complex-glycosylated and core-glycosylated forms of the NKCC2 protein (2, 43). To further confirm this, we mutated the two predicted glycosylation sites, Asn-442 and Asn-452 to glutamine, and assessed the effect of these mutations on NKCC2 glycosylation by immunoblot. As shown in Fig. 1*B*, elimination of both Asn-442 and Asn-452 resulted in the complete loss of the upper band with a lower band around 120 kDa remaining, clearly demonstrating that the observed bands are specific to Myc-NKCC2 fusion protein.

To further document the detection of Myc-NKCC2 protein in our cells and analyze its subcellular distribution, confocal microscopy imaging of indirect immunofluorescence was performed. As shown in Fig. 2*A*, Myc-NKCC2 staining (*green*) was

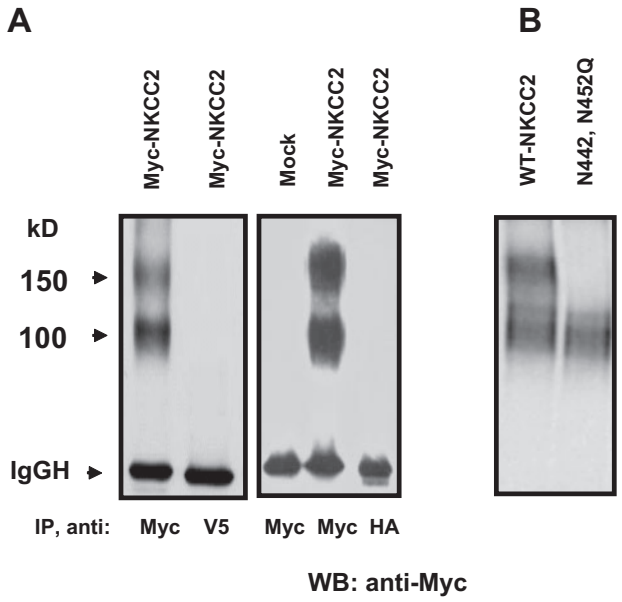

FIGURE 1. **NKCC2 protein expression in renal epithelial cells.** *A,* expression of Myc-NKCC in transiently transfected OKP cells. Cell lysates from OKP cells were subjected to immunoprecipitation (*IP*) using either mouse anti-Myc antibody, anti-V5 antibody, or anti-HA antibody. Samples were then reduced (boiled in β-mercaptoethanol), evaluated via 7.5–10% SDS-PAGE, and immunoblotted with anti-Myc antibody. Myc-NKCC2 protein was detected as two bands, one around 160 kDa and the other around 120 kDa. *IgGH,* the heavy chain of immunoglobulin G. *B,* immunoblot analysis of cell lysates from OKP cells transiently transfected with wild type NKCC2 or N442C,N452Q mutant. Elimination of both Asn-442 and Asn-452 resulted in the complete loss of the upper band, the complex-type glycosylated form of NKCC2. *WB*, Western blot.

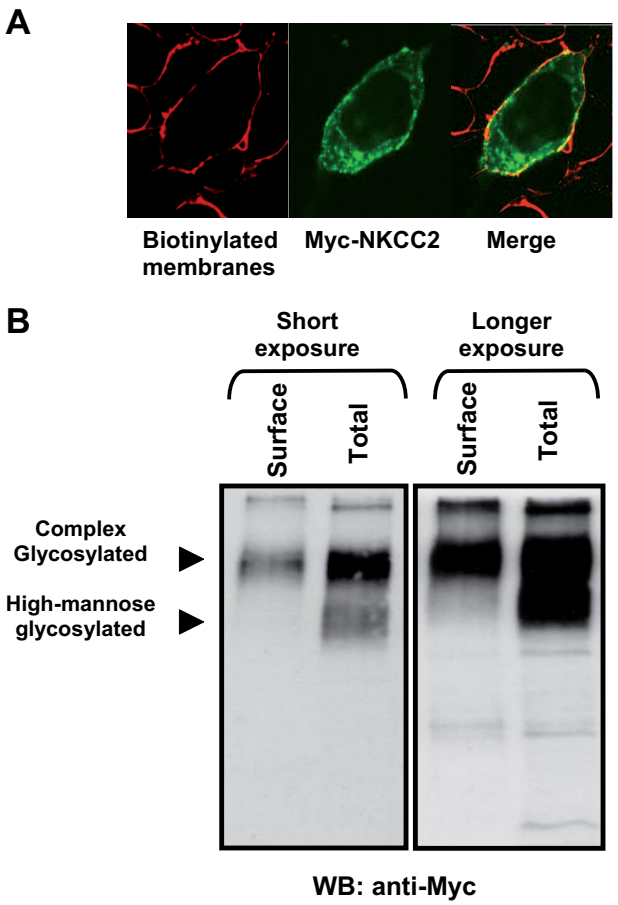

FIGURE 2. **NKCC2 surface expression.** *A,* immunolocalization of Myc-NKCC2. MKTAL cells membranes were biotinylated at 4 °C. Then the monolayers were fixed and stained for Myc-NKCC2 fusion protein (Cy-2) and cell surface biotin (avidin-Cy3). The stained specimens were evaluated by confocal microscopy. Optical sections (*XY*) at the cell surface are depicted for the Cy2 channel (*green*), Cy3 channel (*red*), and a merged channel. The *yellow* color indicates that Myc-NKCC-2 co-localizes with biotinylated proteins in the cell surface indicating adequate targeting of the co-transporter to the plasma membrane. *B,* confluent cells were biotinylated at 4 °C with the cleavable biotinylation reagent sulfo-NHS-SS-biotin. Biotinylated proteins were recovered from cell extracts by precipitation with streptavidin-agarose. NKCC2 on the cell surface was detected by Western blotting with Myc antibody. An aliquot of the total cell extract from each sample was also run on a parallel SDS gel and Western blotted (*WB*) to provide a measure of total NKCC2 expression. The biotinylated protein fraction contained only the complex-type glycosylated fraction (160 kDa) of Myc-NKCC2 indicating that the mature NKCC2 component is complex-type glycosylated.

detected intracellularly and at the cell periphery confirming NKCC2 protein expression. More importantly, Myc-NKCC2 staining co-localized with biotinylated cell-surface proteins (Fig. 2*A, red*), indicating adequate targeting of the co-transporter to the plasma membrane under these conditions. To further confirm this, we examined NKCC2 surface expression using surface biotinylation. Surface membrane proteins were biotinylated by reaction with sulfo-NHS-SS-biotin and isolated by precipitation with streptavidin-bound agarose. Myc-NKCC2 protein was then identified by immunoblot using anti-Myc antibody (Fig. 2*B*). Interestingly, in contrast to the total cell lysate, the biotinylated protein fraction contained only the complex-type glycosylated fraction of Myc-NKCC2. Thus, the mature NKCC2 component is complex-type glycosylated. Only this fraction of NKCC2 pool was able to reach the cell surface. The high mannose-type core glycosylated fraction of NKCC2 present in the cell lysate represents the immature endoplasmic reticulum portion of the NKCC2 pool.

Identification of Aldolase B as an Interactor with the C Terminus of NKCC2 by Yeast Two-hybrid Screen—To uncover the protein binding partners of NKCC2, we performed yeast two-hybrid to screen a human kidney cDNA expression library, using a series of bait fragments spanning the predicted cytoplasmic C terminus (residues 661–1095) of murine NKCC2. We named these regions C1-term, C2-term, and C3-term (Fig. 3*A*). In this study, we describe the data obtained with C1 (NKCC2 C1-term), the fragment encompassing the first 108 AA (residues 661–768). Among the identified clones, five matched the sequence of human aldolase B. These clones contained overlapping and partial sequences of aldolase B (residues 1–364), and ranged in length from residues 110–364 to 190–364 (Fig. 3*B*), indicating that the 174 AA at the C terminus of aldolase B are sufficient for the observed interaction.

Because the yeast two-hybrid assay sometimes identifies false positive clones, we carried out a series of experiments to verify and confirm the specificity of the interaction between aldolase and NKCC2 proteins (Fig. 3*C*). It is noteworthy that all the constructs used in these experiments are issued from the yeast two-hybrid screening and that the reading frames in the bait and prey plasmids were verified.

To confirm the initial interaction between C1-term and aldolase B, we transformed AH109 yeast cells with the BD-NKCC2 C1-term and AD-aldolase B. After selection for growth on His/Leu/Trp triple dropout plates, positive clones were

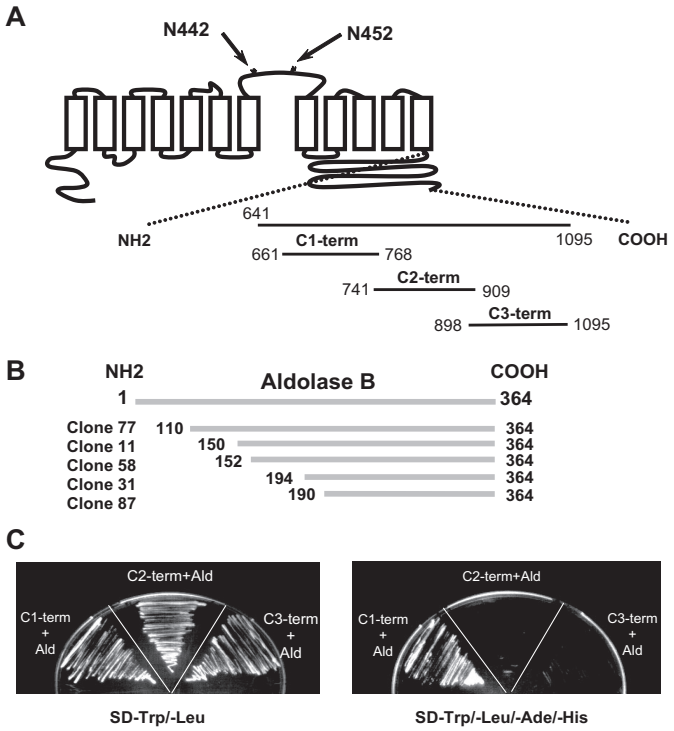

FIGURE 3. **Yeast two-hybrid analysis identifies an interaction between aldolase B and the C1 peptide of the NKCC2 C-terminal part.** *A,* mouse NKCC2 yeast two-hybrid baits constructs. A proposed topology for sodium-coupled chloride co-transporter BSC1/NKCC2 (2). The part of the mouse NKCC2 C terminus was divided into three peptide fragments used as baits for the yeast two-hybrid. Each bait has a common area with the bait that precedes it. These parts have been termed C1-term, C2-term, and C3-term. Asn-442 and Asn-452 are the potential *N*-glycosylation sites. *B,* among the identified clones, five matched the sequence of human aldolase B and contained overlapping and partial sequences of the enzyme. *C,* yeast two-hybrid analysis was performed using the Matchmaker system as described under "Experimental Procedures." The experiment demonstrates that the co-expression of aldolase B and C1-term is required to support the growth of yeast in the absence of tryptophan, leucine, histidine, and adenine in the medium. This experiment also demonstrates the specific interaction between C1-term and aldolase B compared with C2-term and C3-term.

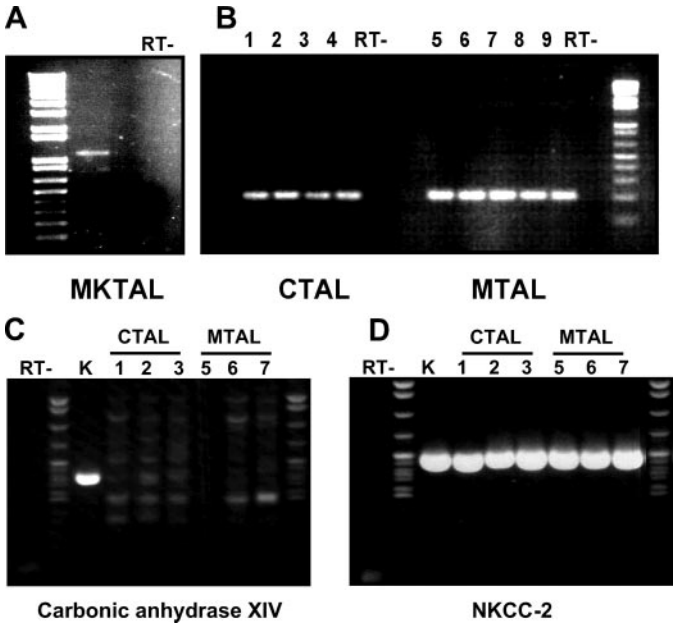

FIGURE 4. **Aldolase B mRNA expression in TAL cells.** Real time PCR and conventional RT-PCRs were carried out using specific primers of aldolase B sequence as described under "Experimental Procedures." *RT−* indicates the negative control of the RT-PCR without transcriptase reverse enzyme. *A,* reaction products from conventional RT-PCR experiments performed on MKTAL cells were separated using 1% agarose gel containing ethidium bromide. An expected band of 1125 bp corresponding to the full-length of aldolase cDNA was obtained. *B,* reaction products obtained from real time RT-PCR on medullary (*MTAL*), *lanes 1–4*, and cortical TAL (*CTAL*), *lanes 5–10*, were separated using 2% agarose gel containing ethidium bromide. The expected size of the amplified aldolase band was 204 bp. *C* and *D,* controls for the microdissection experiments; samples used in *lanes 1–3* and *lanes 5–7* were subjected to real time RT-PCR to detect NKCC2 (TAL positive marker) and carbonic anhydrase XIV (negative marker). For each reaction, a positive control was performed using total kidney homogenates (*lane K*).

streaked on Ade/His/Leu/Trp dropout plates. The results confirmed the interaction between NKCC2 C1-term with aldolase B as judged by growth of the AH109 reporter strain on selection medium. No growth was observed when AH109 was transformed with the BD-NKCC2 C1-term and pACT2 empty vector or when AD-aldolase was co-expressed with pGBKT7 empty vector.

To test the specificity of aldolase-NKCC2 C1-term interaction, we used as bait the other two fragments of the NKCC2 C terminus encompassing the intermediate (residues 741–909, C2-term) and the distal regions (residues 898–1095, C3-term) of the NKCC2 C terminus. In contrast to the proximal region, no growth was observed when AH109 was transformed with AD-aldolase and the two other regions of the NKCC2 C terminus (Fig. 3*C*), indicating that the interaction was specific for the first 108 AA of the NKCC2 C terminus. Taken together, these data show that aldolase B interacts specifically with NKCC2, an interaction for which the first 108 AA of NKCC2 C terminus and the last 174 AA of aldolase B C terminus are sufficient.

Real Time RT-PCR Analysis Demonstrates That Aldolase B Is Expressed in TAL Cells—As a prerequisite for establishing physiological relevance of the observed interaction between NKCC2 and aldolase B, both proteins should be co-expressed in the same cells and share overlapping subcellular distributions.

The expression of NKCC2 in TAL cells is well documented and unequivocally demonstrated (1, 2). By contrast, it has been generally assumed until recently that the expression of aldolase B in the kidney is restricted to the cortex and more precisely to the proximal tubules (44–46). However, recent studies revealed that aldolase B is also expressed in the renal medulla (47). Most interestingly, Lu *et al.* (25) indicated that in mouse kidney, aldolase B protein is detected in the cytoplasm of the thick ascending limb and in the Bowman capsule. To confirm the expression of aldolase B in kidney TAL, we checked for the presence of its transcript in native TAL cells and in a mouse kidney TAL cell line (MKTAL) using real time RT-PCR and conventional RT-PCR, respectively.

As shown in Fig. 4*A*, conventional RT-PCR on MKTAL cells using a set of specific primers for aldolase B yielded a single band of 1125 bp, corresponding to the expected size of full-length aldolase B cDNA. No PCR product was obtained when reverse transcriptase was omitted from the RT reaction.

For real time RT-PCR, each reaction was performed on the equivalent of 0.25 mm of microdissected medullary (MTAL) and cortical TAL tubules. After amplification using a set of specific primers for aldolase B, melting curve analysis revealed the expression of a single reaction product that, when separated using agarose gel electrophoresis (Fig. 4*B*), revealed as well a

single reaction product of the corresponding expected size (204 bp) indicating the expression of aldolase B in native medullary and cortical TAL cells. To ensure that RT-PCR products were specifically because of amplification of aldolase B transcript from TAL cells, and not because of contamination with other renal segments expressing aldolase B such as the proximal tubule, samples used in Fig. 4*B*, *lanes 1–3* and *lanes 5–7*, were subjected to real time RT-PCR to detect NKCC2 and carbonic anhydrase XIV. NKCC2 was used as positive marker for TAL cells, whereas carbonic anhydrase XIV, a protein strongly expressed in the proximal tubule (48), served as a negative marker for TAL cells (48). For each reaction, a positive control was performed using total kidney homogenates. As can be seen in Fig. 4, RT-PCR analysis on the tested samples demonstrated the expression of NKCC2 (Fig. 4*D*) but not carbonic anhydrase XIV (Fig. 4*C*), clearly confirming that aldolase B RT-PCR product shown in Fig. 4*A* did originate from TAL cells. All together, these data clearly show that aldolase B is co-expressed with NKCC2 in both cortical and medullary TAL of the kidney.

Endogenous Aldolase Protein Interacts and Co-localizes with NKCC2—Heterologous expression of certain proteins may induce nonspecific aggregation with other proteins because of overexpression. To minimize this possibility, we next tested whether endogenous aldolase B protein and NKCC2 interact in cultured cells. As mentioned above, aldolase B protein expression in renal proximal tubule cells is unequivocally demonstrated (44–46). Given that OKP cells are an excellent model of proximal tubule cells (41, 42) and that transient transfection is very efficient in these cells (49, 50), we assumed that they are an appropriate model for testing the ability of NKCC2 to interact with endogenous aldolase protein. To address this, a goat antibody raised against native aldolase protein was used. Of note, the efficiency of this goat anti-aldolase antibody in detecting aldolase B protein was verified by immunoprecipitation and Western blot analysis of cells transiently transfected with aldolase B-V5 construct. Indeed, the same band, ~45-kDa band, consistent with predicted molecular mass of aldolase B protein (36–41 kDa) plus a V5 tag (5 kDa) was detected with both antibodies (data not shown) clearly demonstrating the effectiveness of the goat anti-aldolase antibody in recognizing aldolase B protein. Consequently, to document the expression of aldolase protein in OKP cells, we first subjected lysates from these cells to immunoblot analysis using goat anti-aldolase antibody. As shown in Fig. 5*A*, a single protein band around 37 kDa was obtained, corresponding to the expected size band of aldolase B (51). Importantly, the same signal was obtained by Western blot analysis following immunoprecipitation with anti-aldolase antibody (Fig. 5*A*, *lane 2*), further confirming the endogenous expression of aldolase protein in OKP cells. More importantly, immunoprecipitation of endogenous aldolase protein brought down NKCC2 as verified by immunoblotting with anti-Myc antibody demonstrating physical interaction between the two proteins (Fig. 5*B, lane 3*). The interaction appears to be specific because Myc-NKCC2 protein was not detected in control experiments in which immunoprecipitations were carried out using mouse anti-HA (Fig. 5*B, lane 2*) or anti-V5 antibodies (Fig. 1*A*).

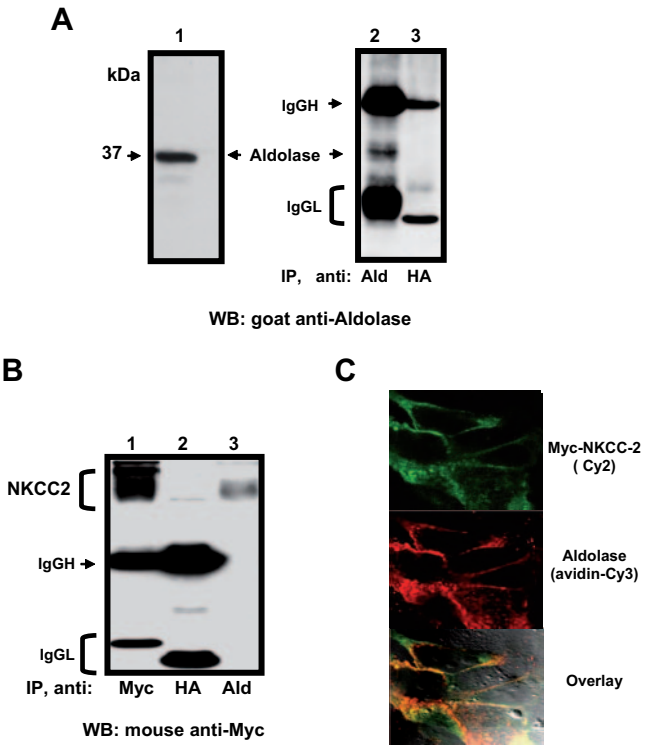

FIGURE 5. **NKCC2 co-localizes and interacts with endogenous aldolase protein.** *A,* aldolase endogenous expression in OKP cells. Cell lysates from OKP cells were subjected to immunoprecipitation (*IP*) using either goat anti-aldolase (*Ald*) antibody or mouse anti-HA antibody (negative control, *upper panel, lane 3*). Samples were then reduced (boiled in β-mercaptoethanol), evaluated via 7.5–10% SDS-PAGE, and immunoblotted with anti-aldolase antibody. A single protein band around 37 kDa was obtained, corresponding to the expected size band of aldolase B. *B,* co-immunoprecipitation of aldolase with full-length NKCC2. Cell lysates from OKP cells transiently expressing myc-NKCC2 were immunoprecipitated with anti-Myc antibody (positive control, *lower panel*, *lane 1*) or anti-HA (negative control, *lower panel*, *lane 2*), or anti-aldolase antibody (*lower panel*, *lane 3*). Co-immunoprecipitated NKCC-2 with aldolase was detected by immunoblotting using anti-Myc (*lower panel*, *lane 3*). *IgGH*, the heavy chain of immunoglobulin G; *IgGL*, the light chain of immunoglobulin G. *WB*, Western blot. *C,* immunofluorescence staining of aldolase and Myc-NKCC2 proteins. OKP cells were double-stained with anti-Myc and anti-aldolase antibodies. Anti-aldolase and anti-Myc antibodies were visualized with a biotinylated anti-goat IgG antibody and Cy3-labeled streptavidin (*red*) and Cy2-labeled anti-mouse (*green*) IgG antibodies, respectively. The *yellow* color (merged image) indicates co-localization of aldolase and NKCC2 proteins.

To further confirm this, the association of NKCC2 with endogenous aldolase protein was examined in intact OKP cells by immunofluorescence confocal microscopy. As shown in Fig. 5*C*, NKCC2 (*green*) largely co-localized with aldolase (*red*), indicating that these two proteins share the same subcellular localization. Taken in concert, these findings clearly indicate that NKCC2 interaction with aldolase B is not an artifact of the yeast two-hybrid system and that an NKCC2 aldolase complex really exists in cells.

Fructose 1,6-Bisphosphate (FBP) Disrupts Aldolase Binding to NKCC2—Aldolase binding can be modulated, in most cases, by the presence of its substrate and products (21, 24, 27, 52, 53). This phenomenon is commonly taken as an indication that a region close to the active site of aldolase participates in the interaction (24, 27, 52, 53). Hence, it was of interest to examine the effect of FBP on aldolase interaction with NKCC2. To accomplish this, 24 h after transfection with Myc-NKCC2,

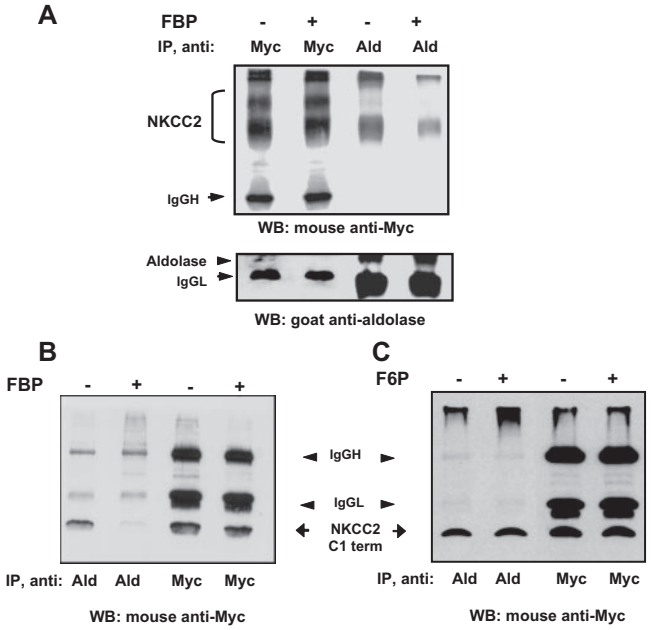

FIGURE 6. **Aldolase binding to NKCC2 is specifically inhibited by fructose 1,6-bisphosphate.** OKP cells were transfected with NKCC2-Myc (*A*) or NKCC2-C1term (*B* and *C*). 24 h after transfection, cells were treated overnight with 5 mM FBP or 5 mM fructose 6-phosphate. They were then subjected to immunoprecipitation (*IP*) using either mouse anti-Myc antibody or goat anti-aldolase (*Ald*) antibody. The resultant immunopellets were subjected to SDS-PAGE on a 7.5% polyacrylamide gel and then analyzed by immunoblotting using mouse anti-Myc monoclonal antibody or goat anti-aldolase antibody. FBP presence disrupted NKCC2-aldolase interaction (*A, upper and lower panels*, and *B*). In contrast to FBP, the structurally similar compound fructose 6-phosphate (*F6P*) had no effect on the interaction (*C*) indicating that FBP effect is specific. *IgGH*, the heavy chain of immunoglobulin G; *IgGL*, the light chain of immunoglobulin G. *WB*, Western blot.

intact cells were treated overnight with 5 mM FBP. Of note, several previous studies provided compelling evidence that FBP can be taken up by intact cells (54–57) in a concentration-dependent manner with a narrow range of 5–10 mM in which FBP is the most effective (54, 55). As illustrated in Fig. 6*A*, treatment of cells with FBP had no effect on total cellular amount of NKCC2 (Myc immunoprecipitates). In contrast, FBP strikingly reduced the amount of NKCC2 proteins recovered from aldolase immunoprecipitates (Fig. 6*A*, *upper panel*). To perform the reciprocal experiment, we repeated the blots in Fig. 6*A* by subjecting the same samples to Western blot analysis using anti-aldolase antibody. A single band around the 37-kDa protein, corresponding to the expected size of aldolase protein, was co-immunoprecipitated in the presence of Myc antibody (Fig. 6*A, lower panel*) but was detectable only after a long exposure. Importantly, in the presence of FBP, the aldolase band was not detected in Myc immunoprecipitates, suggesting disruption of aldolase/NKCC2 co-association. Collectively, these data not only confirm NKCC2 interaction with endogenous aldolase protein but also suggest that a region close to the active site of aldolase participates in its interaction with NKCC2.

Given that the bait used in the two-hybrid system screening was only the first 108 AA of the NKCC2 C terminus (C1-term region), we also tested the ability of this region to interact *in vivo* with endogenous aldolase protein in OKP cells. Cells were co-transfected with plasmid encoding NKCC2 C1-term N-terminally tagged with the Myc epitope. Immunoprecipitations were carried out using mouse anti-Myc antibody and goat anti-aldolase antibody to immunoprecipitate NKCC2 C1-term and aldolase B proteins, respectively. As illustrated in Fig. 6*B*, immunoprecipitation of aldolase protein with goat anti-aldolase antibody brought down Myc-NKCC2 C1-term fusion protein as verified by immunoblotting with anti-Myc demonstrating association between the two proteins. Again, cells treatment with 5 mM FBP clearly affected aldolase binding as judged by NKCC2 C1-term content in aldolase immunoprecipitates in the presence and the absence of FBP. Finally, to check the specificity of FBP effect on the interaction, we used fructose 6-phosphate, a compound structurally similar to FBP but not an aldolase substrate. In contrast to FBP, fructose 6-phosphate had no effect on the interaction between NKCC2 C1-term and aldolase (Fig. 6*C*). Hence, these findings provide additional evidence to that in Fig. 5 that aldolase B interacts with the NKCC2 C terminus in renal epithelial cells and that the binding site for NKCC2 involves the catalytic domain of the enzyme.

Aldolase Binding Reduces NKCC2 Surface Expression—Aldolase is a protein associated with the actin cytoskeleton and can cross-link actin fibers (22, 23). Because actin cytoskeleton has been implicated in the regulation of Na-K-Cl co-transport in mouse kidney cultured TAL cells (58), we therefore sought to study the effect of aldolase binding on NKCC2 surface expression. To address this, we first checked the effect of aldolase B overexpression on NKCC2 subcellular distribution in MKTAL cells. Toward that, we generated two new plasmid constructs in which NKCC2 was tagged (N-terminally) with GFP and aldolase B with V5. We then co-expressed GFP-NKCC2 and aldolase-V5 fusion proteins in MKTAL cells and visualized with confocal microscopy their subcellular localization (Fig. 7). Similarly to Myc-NKCC2, when expressed alone, GFP-NKCC2 fusion proteins were found distributed primarily in the plasma membrane, appearing as a rim of fluorescence around the surface of the cell or in intracellular compartments. To our surprise, co-transfection of GFP-NKCC2 with aldolase apparently resulted, in most cases (compare *A* and *B* and *C* to *D, F* and *G*) in an alteration of subcellular distribution of NKCC2 protein. Indeed, when NKCC2 was co-expressed with aldolase, a significant fraction of total NKCC2 appeared, most of the time, to be retained in the cytoplasm where it exhibited excellent co-localization with aldolase B. Although these findings are essentially qualitative, they do suggest that aldolase binding might alter NKCC2 trafficking to the plasma membrane. We therefore sought to study, in a more quantitative fashion, the effect of aldolase on NKCC2 surface expression using cell surface biotinylation.

To address this, we transfected Myc-NKCC2 in the absence (empty vector) or the presence of aldolase B-V5 in MKTAL or OKP cells, and we examined NKCC2 surface expression using surface biotinylation. Again, surface membrane proteins were biotinylated by reaction with sulfo-NHS-SS-biotin and isolated by precipitation with streptavidin-bound agarose. It is worth emphasizing that control and experimental studies are always done in parallel on the same day.

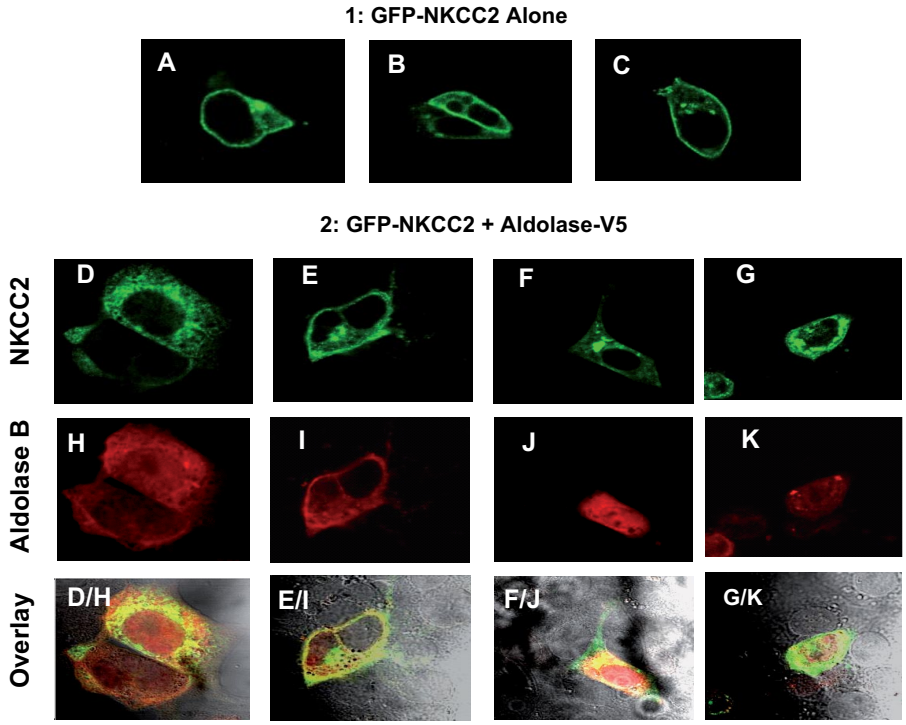

FIGURE 7. **Effect of aldolase B co-expression on NKCC2 protein subcellular distribution.** Immunofluorescence confocal microscopy showing distribution of NKCC2 and aldolase B in MKTAL cells. MKTAL cells were transfected with pEGFP-NKCC2 (*green*) alone (*A–C*) or with pV5-aldolase B (*D–K*). pV5-aldolase B (*red*) was revealed with anti-V5, conjugated with Texas Red-coupled secondary antibodies. *D/H, E/I, F/J,* and *G/K* are merged images, with *yellow* representing precise co-localization.

We documented earlier (Fig. 2) that Myc-NKCC2 fusion proteins are correctly delivered to the membrane in OKP and MKTAL cells and that only the complex-glycosylated form (mature, 160–170 kDa) is able to reach the cell surface. Under biotinylation conditions, cells membrane may become leaky. Hence, in all experiments, the absence of high mannose type NKCC2 (120 kDa) was used as an indication of membrane integrity. As shown in Fig. 8, *A* and *B*, overexpression of aldolase B caused 50 and 35% decrease in cell surface NKCC2 protein in MKTAL ($n = 7$, $p < 0.006$) and OKP cells ($n = 4$, $p < 0.003$), respectively. Importantly, aldolase-induced decrease in NKCC2 surface expression occurred in the absence of a decrease in total cellular amount of NKCC2 (Fig. 8, *A* and *B*) excluding the possibility of nonspecific effects because of protein overexpression in the heterologous expression system we used. This conclusion is further supported by the observation that co-transfecting aldolase with another TAL protein, the endothelin-B receptor, had no effect on the surface expression of the latter (data not shown), indicating that the action of aldolase was specific for NKCC2. Taken in concert, these data suggest the observed decrease in NKCC2 surface expression was because of a subcellular redistribution of the co-transporter.

FBP Prevents Aldolase-induced Down-regulation of NKCC2 Surface Expression—Given that aldolase binding to NKCC2 is modulated by FBP (Fig. 6), we tested the effect of this molecule on aldolase-induced decrease in NKCC2 surface expression. To this end, 24 h after transfection with Myc-NKCC2 in the absence or the presence of aldolase-V5, MKTAL cells were treated overnight with 5 mM FBP as described above. As shown in Fig. 9, in the absence of FBP, aldolase B overexpression caused a 71% decrease ($p < 0,05$) in NKCC2 surface expression. By contrast, the presence of FBP abolished the aldolase effect on NKCC2 surface expression (Fig. 9). Interestingly, in the absence of aldolase co-expression, cells treatment with 5 mM FBP also produced a small but significant increase in NKCC-2 surface level (Fig. 9, compare *lanes 1* with *3, 5* with *7,* and *9* with *11*), which is consistent with interaction of NKCC2 with endogenously expressed aldolase protein. Again, these findings strongly suggest that the catalytic domain of aldolase is involved in its interaction with NKCC2 and thus in aldolase-induced down-regulation of the co-transporter surface expression. Most importantly, they further support the notion that the decrease in NKCC2 surface expression was a result of a protein-protein interaction involving aldolase B.

Aldolase Binding Reduces NKCC2 Activity—In light of the effect of aldolase binding on the NKCC2 surface level, we sought to determine whether this was associated with a decrease in NKCC-2 co-transport activity. To address this, we first verified whether Myc-NKCC2 fusion protein expressed at the cell plasma membrane is functional. Na-K^+(NH_4^+)-2Cl transport activity was assessed by estimating the rate of intracellular acidification caused by entry into the cells of NH_4^+ via this transport mechanism after abrupt application of 20 mM NH_4Cl to the cells (31, 32, 59). Importantly, previous studies conducted in MTAL (31, 32) and OK cells (60) clearly demonstrated that neither Na/H (NH_4^+) exchanger nor Na-K(NH_4^+)-ATPase are involved in the NH_4^+-induced intracellular acidification observed under these experimental conditions. More importantly, Chen and Kempson (60) reported that under control conditions, NH_4^+ entry into OK cells occurs mainly via a barium inhibitable component. Therefore, to determine specifically whether OKP cells transfected with Myc-NKCC2 (OKP/Myc-NKCC2) express a functional co-transporter at the plasma membrane, all our experiments were performed in the presence of 10 mM $BaCl_2$ (see "Experimental Procedures"). The behavior of the pH_i of OKP/Myc-NKCC2 cells after the addition of 20 mM of NH_4Cl to the extracellular medium is illustrated in Fig. 10. Cells first rapidly alkalinize and then recover to a final pH_i, which is below resting levels. The initial rate on intracellular pH recovery (dpH_i/dt), which is exclusively because of NH_4^+ entry (31, 32), was measured over the first 20 s of records as reported earlier (31, 32). As illustrated in Fig. 10, *A* and *D*, the NH_4^+-induced initial rate of pH_i recovery was 6-fold faster in OKP cells expressing Myc-NKCC2 than in mock control cells ($p < 0.05$, $n = 3$), which is

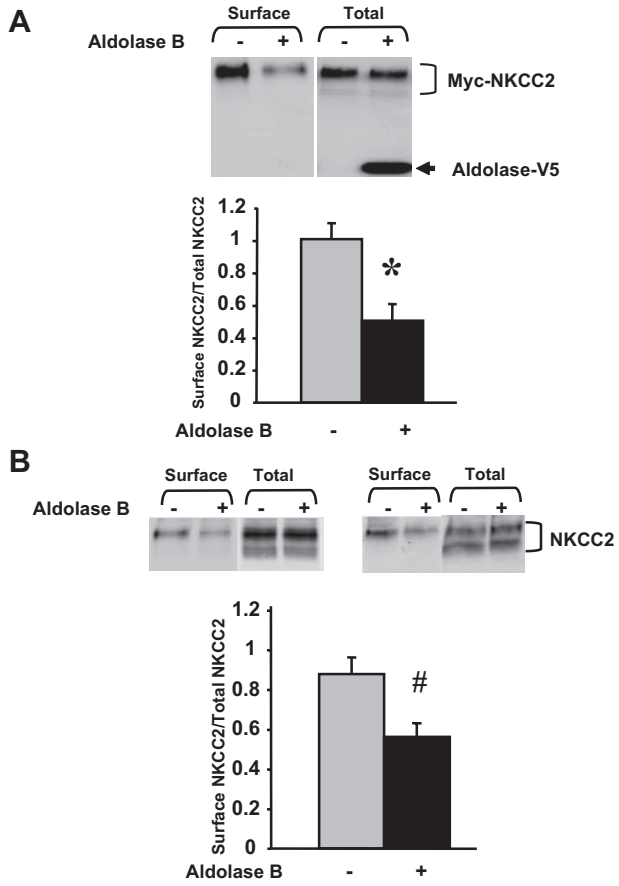

FIGURE 8. **Aldolase B decreases the amount of NKCC2 from the cell surface.** MKTAL (*A*) and OKP (*B*) cells were co-transfected with NKCC2-Myc and the empty vector or with aldolase B-V5 cDNAs as indicated (+). Confluent cells were biotinylated at 4 °C with the cleavable biotinylation reagent sulfo-NHS-SS-biotin. Biotinylated proteins were recovered from cell extracts by precipitation with streptavidin-agarose. NKCC2 on the cell surface was detected by Western blotting using Myc antibody. An aliquot of the total cell extract from each sample was also run on a parallel SDS gel and Western blotted to provide a measure of total NKCC2 expression. Densitometric analysis of total and cell surface NKCC2 is shown as the ratio of biotinylated NKCC2 to total. *, $p < 0.006$; #, $p < 0.005$.

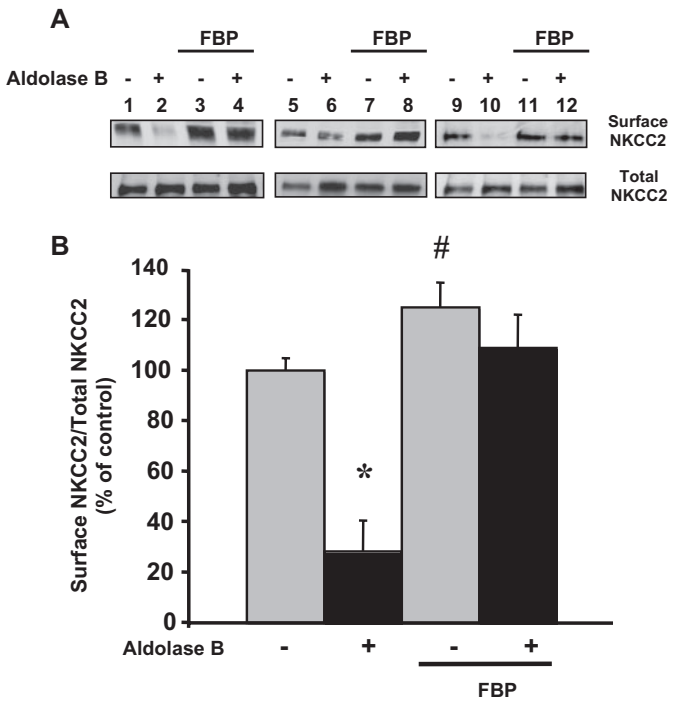

FIGURE 9. **Effect of fructose 1,6-bisphosphate on aldolase B-induced down-regulation of cell surface NKCC2 protein.** MKTAL cells were transfected with Myc-NKCC2 and/or aldolase B-V5 cDNAs as indicated (+). *A*, 24 h after transfection, cells were treated overnight with 5 mM FBP and then biotinylated from the cell surface. Biotinylated proteins were recovered from cell extracts by precipitation with streptavidin-agarose, and NKCC2 on the cell surface was detected by Western blotting using anti-Myc antibody. An aliquot of the total cell extract from each sample was also run on a parallel SDS gel and immunoblotted with anti-Myc antibody to provide a measure of total NKCC2 expression. *B*, densitometric analysis of total and cell surface NKCC2 (ratio of biotinylated NKCC2 to total) from untreated control cells and cells treated with FBP. Data are expressed as percentage of control ± S.E. *, $p < 0.05$; #, $p < 0.05$ when compared with control cells in the absence of aldolase co-expression.

consistent with the presence of a functional Myc-NKCC2 protein. To study the effect of aldolase binding on this Na-K(NH_4^+)-Cl co-transporter, OKP cells were transfected with Myc-NKCC2 in the absence or the presence of aldolase B-V5 proteins. As shown in Fig. 10, *B* and *D*, aldolase co-expression strikingly decelerated the rate of pH_i recovery (−64%, $p < 0.05$, $n = 5$). When cells were treated with 5 mM FBP, aldolase-induced decrease in dpH_i/dt was abolished (−0.019 pH units/min ± 0.03 *versus* −0.016 ± 0.035, control *versus* aldolase transfected cells, $n = 5$). Finally, in the presence of 0.1 mM bumetanide, the initial rate of intracellular pH recovery was suppressed in both groups (Fig. 10, *C* and *D*), which demonstrates that, under our experimental conditions, the NH_4^+-dependent pH_i recovery was because of the activity of Na-K(NH_4^+)-Cl co-transporter. Taken together, these results clearly indicate that aldolase co-expression decreases the activity of Myc-NKCC2 protein. Furthermore, the reduction in NKCC2 levels on the cell surface (Fig. 8 and 9) corresponds well with the changes in NKCC2 transport activity, suggesting that aldolase exerts its effect by causing a redistribution of NKCC2 protein.

DISCUSSION

The Na-K-Cl co-transporter, termed "BSC-1" or "NKCC2," provides the major route for sodium/chloride transport across the apical plasma membrane of the TAL cells of the kidney. Several studies, limited to *Xenopus laevis* oocytes, have addressed various aspects of NKCC2 regulation (2, 36). However, little is known about the regulation of NKCC2 in mammalian cells. In this study, we have successfully approached the problem of expressing NKCC2 protein in mammalian cells by tagging its N-terminal tail. Moreover, we have identified aldolase B as a novel interacting partner of the NKCC2 through yeast two-hybrid screening of a human kidney cDNA library. The data indicated that aldolase B interacts specifically with the first 108 AA of the NKCC2 C terminus. This interaction was confirmed in transfected cells by co-immunoprecipitation experiments and dual immunolabeling fluorescence microscopy. In addition, we demonstrated that aldolase B overexpression promotes NKCC2 retention within the cell, thus decreasing its abundance at the cell surface and its co-transport activity.

The NKCC2 protein is encoded by the *SLC12A1* gene. The cDNA encoding this co-transporter was identified in mamma-

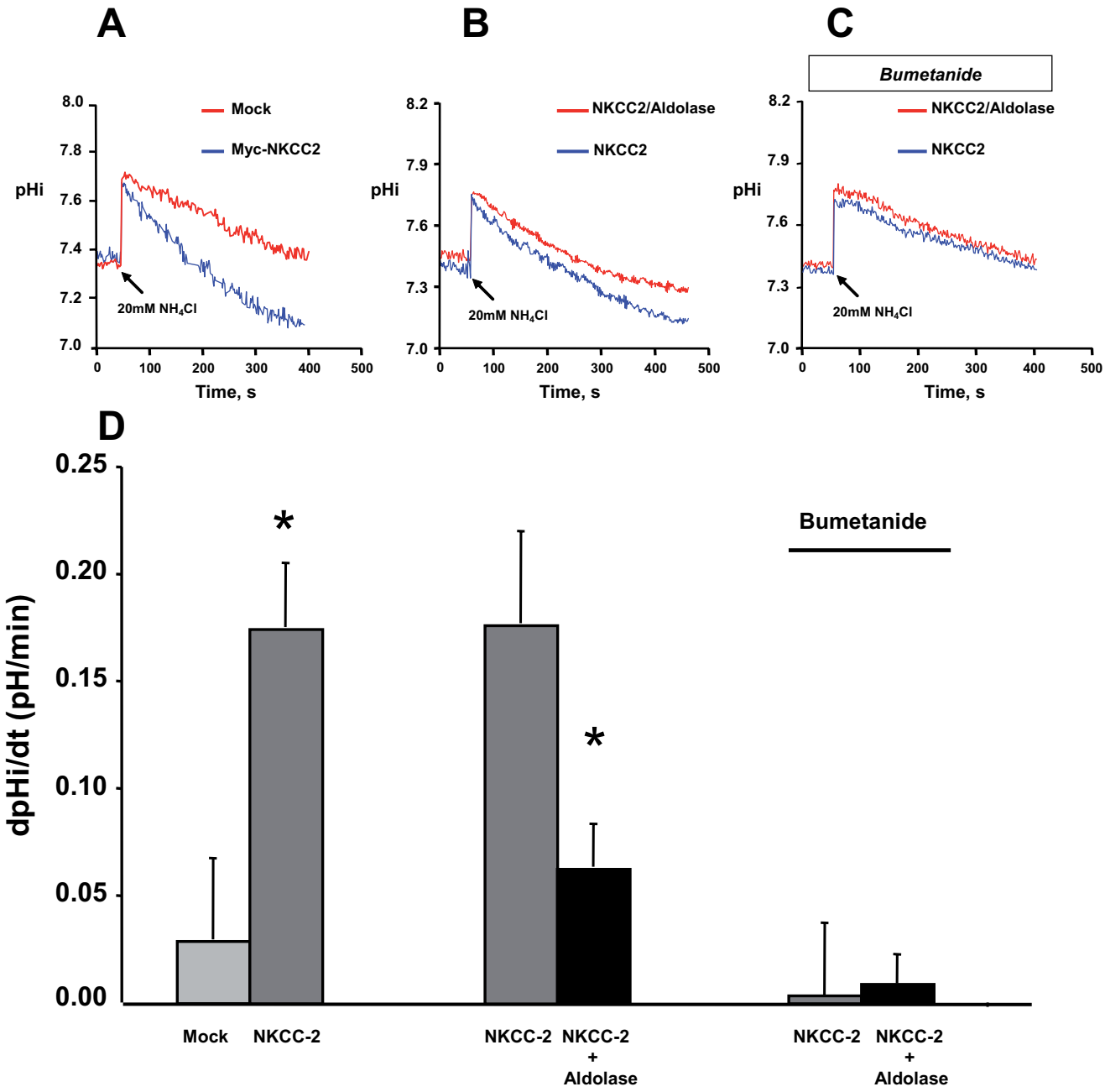

FIGURE 10. **Measurement of Na-K(NH_4^+)-Cl co-transport activity in OKP cells expressing Myc-NKCC2.** Intracellular pH was measured in confluent monolayers of OKP cells as described under "Experimental Procedures." The *arrow* indicates replacement with medium containing 20 mM NH_4Cl (isosmotically substituted for NaCl). *A,* Na-K(NH_4^+)-Cl co-transport activity in OKP cells expressing myc-NKCC2 (*blue*) compared with mock-transfected cells (*red*). *B,* effect of aldolase co-expression (*red*) on NKCC2 activity. *C,* effect of aldolase co-expression on NKCC2 activity in the presence of 0.1 mM bumetanide. Results of representative experiments are shown. *D,* mean initial rate of pH_i recovery (dpH_i/dt) from and NH_4^+-induced alkaline load. Each *bar* represents the mean ± S.E. rates of cell pH recovery (dpH_i/dt, pH units/min) under different experimental conditions (Mock cells, OKP cells expressing Myc-NKCC-2, OKP cells co-transfected with NKCC2 and aldolase B, OKP cells co-transfected with NKCC2 and aldolase B in presence 0.1 mM bumenatide). *, $p < 0.05$.

lian kidney in 1994 (3, 34). Despite this, efforts to achieve stable expression of NKCC2 protein in mammalian cells have been fruitless (34–36), in contrast to the success in expressing NKCC-1 and the other cation chloride co-transporters in HEK293 and Madin-Darby canine kidney cells (61, 62). As a consequence, considerably less is known about the cell biology and post-transcriptional regulation of NKCC2 than the other key renal transport proteins. Interestingly, Isenring *et al.* (35, 63) were able to express an NKCC2-NKCC-1 chimera, in which the 5′-untranslated region and cDNA encoding the first 104 amino acids of rabbit NKCC2A were replaced with the corresponding region from human NKCC1. In addition, Payne and Forbush (34) reported that when the proximal region of the NKCC2 N terminus (the first 105 AA) was deleted, immunoreactive proteins were detected in transiently transfected cells. Based on these observations, we speculated that the N-terminal domain of NKCC2 plays a crucial role in governing the stability of the co-transporter protein. In support of this idea, numerous reports showed evidence that the N-terminal tail plays an important role(s) in regulating the protein stability (37–40, 64).

Most importantly, they demonstrated that the degradation of certain proteins could be blocked following fusion of the Myc tag to their N terminus. Hence, we anticipated that we could successfully express the NKCC2 protein by tagging its N-terminal domain with Myc. Mammalian expression systems offer considerable advantages in reproducibility and in the ability to carry out assays under a large number of conditions. Thus, the NKCC2 protein expression in mammalian cells, described here for the first time, should provide a powerful tool to study and understand the molecular mechanisms underlying the co-transporter expression and regulation in renal epithelial cells.

The apical localization of several ion transport systems appears to depend upon protein-protein interactions involving their extreme C terminus. The apical cystic fibrosis transmembrane regulator chloride channel, for example, interacts with several proteins, including CAL, CAP70, and NHERF (65–67). The deletion of the last three residues of the cystic fibrosis transmembrane regulator C terminus prevents these interactions and results in basolateral accumulation of the mutant protein. The apical Na-P_i co-transporter of the renal proximal tubular brush border also appears to owe its apical distribution in large measure to PDZ interactions mediated through its C-terminal tail (68). By contrast, virtually nothing is known about the underlying molecular mechanisms that control membrane sorting of NKCC2. Accordingly, identifying proteins that interact with the C-terminal tail of NKCC2 should help to determine the mechanism of regulated NKCC2 trafficking. With regard to the NKCC2 C terminus, it has been reported that the murine renal specific Na-K-2Cl co-transporter gene *Slc12A1* exhibits two spliced isoform products that differ at the C terminus (30). However, the full-length isoform (L-NKCC2) appears to be, functionally, the main renal Na-K-Cl co-transporter that provides the apical pathway for vasopressin-regulated NaCl transport across the TAL (69–71). Because the C-terminal domain of L-NKCC2 is the predominant cytoplasmic region (3), it is likely to be a major factor in the trafficking of the NKCC2 protein. Therefore, we used a series of bait fragments spanning the predicted cytoplasmic C terminus (residues 661–1095) of long murine NKCC2 fused to the *GAL4* DNA binding domain to probe a human kidney cDNA library for interacting partners by using the yeast two-hybrid system. In this study, we describe results obtained with one of the fragments encompassing the first 108 AA (residues 661–768). These results identified fructose 1,6-bisphosphate aldolase B, as a specific binding partner of the NKCC2 C terminus.

Fructose 1,6,bisphosphate aldolase B is a key enzyme of the gluconeogenic glycolytic pathway (18). Mutations in the human aldolase B gene that result in diminished aldolase B activity cause the autosomal recessive disease, hereditary fructose intolerance (72, 73). Of note, there are three known isoforms of aldolase, A, B, and C, that are derived from distinct genes (74) and whose deduced amino acid sequences share 85% homology. Interestingly, aldolase was found to be present in cells in much higher concentrations than needed for catalysis suggesting that it might be involved in other cellular activities unrelated to its primary function. In support of this idea, it has been reported that aldolase appears as an interacting protein in an increasing number of processes. Aldolase interacts with calmodulin (20, 75) and phospholipase D_2 (21) and therefore may modulate signal transduction pathways. Aldolase is also an actin-binding protein that exhibits a dynamic interaction with the cytoskeleton (22, 23). Importantly, aldolase interacts with the H^+-ATPase (25, 26) and GLUT4 (27), two proteins regulated by intracellular trafficking. More importantly, it has been suggested that aldolase via its interaction with cytoskeleton functions as a scaffolding protein and plays a crucial role in regulated vesicles exocytosis. Indeed, Kao *et al.* (27) provided compelling evidence for a specific role of aldolase in the insulin stimulation of GLUT4 translocation in adipocytes. In this study, we showed evidence for a specific binding of aldolase B to NKCC2. We observed that NKCC2 interaction with aldolase B is specific for the proximal region of the NKCC2 C terminus. Indeed, the two-hybrid system data showed that aldolase B does not interact with the other regions of the NKCC2 C terminus. Importantly, using co-immunoprecipitation, we were able to detect the interaction *in vivo*, of full-length NKCC2 protein and NKCC2 C1-term with endogenous aldolase protein in OKP cells. Most importantly, we demonstrated that aldolase binding is involved in the regulation of NKCC2 intracellular trafficking.

Under basal conditions, NKCC2 is expressed in the apical plasma membrane and in intracellular vesicles of TAL cells (9). Using immunohistochemistry, we showed similar subcellular localization of Myc-NKCC2 and GFP-NKCC2 fusion proteins in transiently transfected TAL cells. Indeed, in cells expressing NKCC2 alone, the co-transporter was detected at the cell surface and in intracellular compartments. In contrast, in cells co-transfected with NKCC2 and aldolase, we observed an intracellular accumulation of NKCC2 and a consequent reduction in the expression of NKCC2 on the cell surface. Indeed, upon aldolase overexpression, a significant fraction of NKCC2 appears to be retained within the cell where it exhibited an excellent overlap with aldolase immunolabeling. These data suggested that aldolase binding alters NKCC2 trafficking to the cell surface. To confirm this observation, we used surface biotinylation and showed that the co-transporter expression at the cell surface was reduced up to 71% upon aldolase B co-expression. Moreover, we showed that the decrease in NKCC-2 surface expression was associated with a decrease in its co-transport activity. Interestingly, aldolase-induced down-regulation of NKCC-2 surface level occurred in the absence of a decrease in total cellular NKCC2 abundance suggesting that the decrease in the amount of cell surface NKCC2 was because of a redistribution of the co-transporter from the plasma membrane to intracellular vesicular stores.

The precise molecular mechanisms underlying the effect of aldolase on NKCC2 surface expression remain to be resolved. Aldolase-induced down-regulation of NKCC2 membrane abundance could be attributed to a decrease of NKCC2 exocytosis to the apical membrane and/or to an increase of NKCC2 endocytosis. Additional experimentation will be required to distinguish between these possibilities. However, based on a recent study conducted by Lundmark and Carlsson (53), we favor the hypothesis that aldolase decreases NKCC2 exocytosis. Indeed, similar to our findings that aldolase affects NKCC2 trafficking, the authors of the study showed that sorting nexin 9

(SNX9)-dependent recruitment of dynamin-2 (Dyn2) to the membrane is regulated by an interaction between SNX9 and aldolase. SNX9 functions as a mediator of Dyn2 recruitment to membranes in cells. Aldolase binding to SNX9 blocks its membrane binding activity and thus prevents Dyn2 recruitment to the membrane. Importantly, aldolase effect on Dyn2 translocation to the membrane is inhibited by the presence of aldolase substrate or products, as we also found for NKCC2 in this study. Indeed, our results showed that in the presence of FBP, aldolase binding was disrupted, and aldolase B overexpression had no further effect on NKCC2 surface expression and co-transport activity. Thus, it is tempting to speculate that SNX9-aldolase interaction is also involved in an aldolase effect on NKCC2. Further experiments should determine whether the interaction of NKCC2 with aldolase B indeed involves SNX9 or other intermediary regulatory proteins. In this regard, the affinity of aldolase for actin (24, 76) and the involvement of actin cytoskeleton in the regulation of Na-K-Cl co-transport in TAL cells (58) opens the possibility for a key role of actin in aldolase effect on NKCC2 surface expression.

Identifications of proteins that interact with CCC co-transporters and thereby regulate and mediate their expression are important to understand their differential physiological functions. To the best of our knowledge, this is the first study identifying a protein partner of NKCC2 that plays a role in its trafficking to the cell membrane in mammalian cells. Although our study was conducted in cell culture, it is likely that such interaction could also take place in native TAL cells and play a crucial role in the regulation of NKCC2 targeting to the apical membrane, in particular by vasopressin. Indeed, generation of cAMP by hormones such as AVP activates transepithelial transport in the TAL (2). This effect is attributed, at least in part, to an increased NKCC2 translocation to the apical membrane (10, 11). Interestingly, functional expression in *X. laevis* oocytes showed that the C-terminal truncated isoform of *NKCC2* (*S-NKCC2*) reduced L-NKCC2 activity by preventing arrival of the co-transporter to the plasma membrane, an effect prevented by cAMP (71, 77). Most importantly, these studies demonstrated that in the presence of S-NKCC2, but not in its absence, L-NKCC2 surface level is increased by cAMP-dependent protein kinase activation. Similar to S-NKCC2, aldolase co-expression reduces L-NKCC2 surface expression in TAL cells. Interestingly, preliminary studies in our laboratory showed that aldolase action on L-NKCC2 is abrogated by AVP.[3] Thus, it is tempting to speculate that aldolase binding is also involved in AVP-induced exocytosis of NKCC2. One possibility is that aldolase and S-NKCC2 work in concert to create a synergetic effect on L-NKCC2 surface expression. In this model, the absence of cAMP allows aldolase B and S-NKCC2 to reduce NKCC2 surface expression, whereas in the presence of cAMP, down-regulation of NKCC2 surface expression by these two proteins is inhibited.

In summary, using the yeast two-hybrid system, we have identified aldolase B as a novel NKCC2-interacting protein. Co-immunoprecipitation experiments confirmed the interaction in renal epithelial cells. Co-immunofluorescence and biotinylation assays revealed that the interaction of aldolase with NKCC2 results in the retention and accumulation of NKCC2 in the cytoplasm. Therefore, we showed evidence of a new regulatory mechanism governing the apical expression of NKCC2 in renal epithelial cells. Such a mechanism could be a key factor in determining the spatial distribution and the functional regulation of kidney transporters in general and in particular of CCC co-transporters.

[3] B. Benziane, S. Demaretz, N. Defontaine, and K. Laghmani, unpublished data.

REFERENCES

1. Russell, J. (2000) *Physiol. Rev.* **80,** 211–276
2. Gamba, G. (2005) *Physiol. Rev.* **85,** 423–493
3. Gamba, G., Miyanoshita, A., Lombardi, M., Lytton, J., Lee, W. S., Hediger, M. A., and Hebert, S. C. (1994) *J. Biol. Chem.* **269,** 17713–17722
4. Xu, J. C., Lytle, C., Zhu, T. T., Payne, J. A., Benz, E., Jr., and Forbush, B., III (1994) *Proc. Natl. Acad. Sci. U. S. A.* **91,** 2201–2205
5. Delpire, E., Rauchman, M. I., Beier, D. R., Hebert, S. C., and Gullans, S. R. (1994) *J. Biol. Chem.* **269,** 25677–25683
6. Kaplan, M. R., Plotkin, M. D., Lee, W. S., Xu, Z. C., Lytton, J., and Hebert, S. C. (1996) *Kidney Int.* **49,** 40–47
7. Simon, D. B., and Lifton, R. P. (1996) *Am. J. Physiol.* **271,** F961–F966
8. Kurtz, C. L., Karolyi, L., Seyberth, H. W., Koch, M. C., Vargas, R., Feldmann, D., Vollmer, M., Knoers, N. V., Madrigal, G., and Guay-Woodford, L. M. (1997) *J. Am. Soc. Nephrol.* **8,** 1706–1711
9. Nielsen, S., Maunsbach, A. B., Ecelbarger, C. A., and Knepper, M. A. (1998) *Am. J. Physiol.* **275,** F885–F893
10. Gimenez, I., and Forbush, B. (2003) *J. Biol. Chem.* **278,** 26946–26951
11. Ortiz, P. A. (2006) *Am. J. Physiol.* **290,** F608–F616
12. Gagnon, K. B., England, R., and Delpire, E. (2006) *Am. J. Physiol.* **290,** C134–C142
13. Simard, C. F., Daigle, N. D., Bergeron, M. J., Brunet, G. M., Caron, L., Noel, M., Montminy, V., and Isenring, P. (2004) *J. Biol. Chem.* **279,** 48449–48456
14. Piechotta, K., Garbarini, N., England, R., and Delpire, E. (2003) *J. Biol. Chem.* **278,** 52848–52856
15. Darman, R. B., Flemmer, A., and Forbush, B. (2001) *J. Biol. Chem.* **276,** 34359–34362
16. Caron, L., Rousseau, F., Gagnon, E., and Isenring, P. (2000) *J. Biol. Chem.* **275,** 32027–32036
17. Liedtke, C. M., Wang, X., and Smallwood, N. D. (2005) *J. Biol. Chem.* **280,** 25491–25498
18. Yanez, A. J., Ludwig, H. C., Bertinat, R., Spichiger, C., Gatica, R., Berlien, G., Leon, O., Brito, M., Concha, I. I., and Slebe, J. C. (2005) *J. Cell. Physiol.* **202,** 743–753
19. Ali, M., Rellos, P., and Cox, T. M. (1998) *J. Med. Genet.* **35,** 353–365
20. Orosz, F., Christova, T. Y., and Ovadi, J. (1988) *Mol. Pharmacol.* **33,** 678–682
21. Kim, J. H., Lee, S., Lee, T. G., Hirata, M., Suh, P. G., and Ryu, S. H. (2002) *Biochemistry* **41,** 3414–3421
22. Bronstein, W. W., and Knull, H. R. (1981) *Can. J. Biochem.* **59,** 494–499
23. Stewart, M., Morton, D. J., and Clarke, F. M. (1980) *Biochem. J.* **186,** 99–104
24. Wang, J., Morris, A. J., Tolan, D. R., and Pagliaro, L. (1996) *J. Biol. Chem.* **271,** 6861–6865
25. Lu, M., Holliday, L. S., Zhang, L., Dunn, W. A., Jr., and Gluck, S. L. (2001) *J. Biol. Chem.* **276,** 30407–30413
26. Lu, M., Sautin, Y. Y., Holliday, L. S., and Gluck, S. L. (2004) *J. Biol. Chem.* **279,** 8732–8739
27. Kao, A. W., Noda, Y., Johnson, J. H., Pessin, J. E., and Saltiel, A. R. (1999) *J. Biol. Chem.* **274,** 17742–17747
28. Bourgeois, S., Rossignol, P., Grelac, F., Chalumeau, C., Klein, C., Laghmani, K., Chambrey, R., Bruneval, P., Duong, J. P., Poggioli, J., Houillier, P., Paillard, M., Kellermann, O., and Froissart, M. (2003) *Pfluegers Arch.* **446,** 672–683
29. Doucet, A., Katz, A. I., and Morel, F. (1979) *Am. J. Physiol.* **237,** F105–F113

30. Mount, D. B., Baekgaard, A., Hall, A. E., Plata, C., Xu, J., Beier, D. R., Gamba, G., and Hebert, S. C. (1999) *Am. J. Physiol.* **276,** F347–F358
31. Amlal, H., Paillard, M., and Bichara, M. (1994) *J. Biol. Chem.* **269,** 21962–21971
32. Amlal, H., Legoff, C., Vernimmen, C., Paillard, M., and Bichara, M. (1996) *Am. J. Physiol.* **271,** C455–C463
33. Roos, A., and Boron, W. F. (1981) *Physiol. Rev.* **61,** 296–434
34. Payne, J. A., and Forbush, B., III (1994) *Proc. Natl. Acad. Sci. U. S. A.* **91,** 4544–4548
35. Isenring, P., Jacoby, S. C., Payne, J. A., and Forbush, B., III (1998) *J. Biol. Chem.* **273,** 11295–11301
36. Mount, D. B. (2006) *Am. J. Physiol.* **290,** F606–F607
37. Mikalsen, T., Johannessen, M., and Moens, U. (2005) *Int. J. Biochem. Cell Biol.* **37,** 2513–2520
38. Fajerman, I., Schwartz, A. L., and Ciechanover, A. (2004) *Biochem. Biophys. Res. Commun.* **314,** 505–512
39. Breitschopf, K., Bengal, E., Ziv, T., Admon, A., and Ciechanover, A. (1998) *EMBO J.* **17,** 5964–5973
40. Aviel, S., Winberg, G., Massucci, M., and Ciechanover, A. (2000) *J. Biol. Chem.* **275,** 23491–23499
41. Miyauchi, A., Dobre, V., Rickmeyer, M., Cole, J., Forte, L., and Hruska, K. A. (1990) *Am. J. Physiol.* **259,** F485–F493
42. Moe, O. W., Miller, R. T., Horie, S., Cano, A., Preisig, P. A., and Alpern, R. J. (1991) *J. Clin. Investig.* **88,** 1703–1708
43. Paredes, A., Plata, C., Rivera, M., Moreno, E., Vazquez, N., Munoz-Clares, R., Hebert, S. C., and Gamba, G. (2006) *Am. J. Physiol.* **290,** F1094–F1102
44. Saez, D. E., and Slebe, J. C. (2000) *J. Cell. Biochem.* **78,** 62–72
45. Wachsmuth, E. D., Thoner, M., and Pfleiderer, G. (1975) *Histochemistry* **45,** 143–161
46. Vallet, V., Bens, M., Antoine, B., Levrat, F., Miquerol, L., Kahn, A., and Vandewalle, A. (1995) *Exp. Cell Res.* **216,** 363–370
47. McReynolds, M. R., Taylor-Garcia, K. M., Greer, K. A., Hoying, J. B., and Brooks, H. L. (2005) *Am. J. Physiol.* **288,** F315–F321
48. Kaunisto, K., Parkkila, S., Rajaniemi, H., Waheed, A., Grubb, J., and Sly, W. S. (2002) *Kidney Int.* **61,** 2111–2118
49. Laghmani, K., Sakamoto, A., Yanagisawa, M., Preisig, P. A., and Alpern, R. J. (2005) *Am. J. Physiol.* **288,** F732–F739
50. Hu, M. C., Fan, L., Crowder, L. A., Karim-Jimenez, Z., Murer, H., and Moe, O. W. (2001) *J. Biol. Chem.* **276,** 26906–26915
51. Reznick, A. Z., Rosenfelder, L., Shpund, S., and Gershon, D. (1985) *Proc. Natl. Acad. Sci. U. S. A.* **82,** 6114–6118
52. Buscaglia, C. A., Coppens, I., Hol, W. G., and Nussenzweig, V. (2003) *Mol. Biol. Cell* **14,** 4947–4957
53. Lundmark, R., and Carlsson, S. R. (2004) *J. Biol. Chem.* **279,** 42694–42702
54. Ehringer, W. D., Niu, W., Chiang, B., Wang, O. L., Gordon, L., and Chien, S. (2000) *Mol. Cell Biochem.* **210,** 35–45
55. Wheeler, T. J., McCurdy, J. M., denDekker, A., and Chien, S. (2004) *Mol. Cell Biochem.* **259,** 105–114
56. Juergens, T. M., and Hardin, C. D. (1996) *Mol. Cell Biochem.* **154,** 83–93
57. Lazzarino, G., Cattani, L., Costrini, R., Mulieri, L., Candiani, A., and Galzigna, L. (1984) *Clin. Biochem.* **17,** 42–45
58. Wu, M. S., Bens, M., Cluzeaud, F., and Vandewalle, A. (1994) *J. Membr. Biol.* **142,** 323–336
59. Paulais, M., and Turner, R. J. (1992) *J. Clin. Investig.* **89,** 1142–1147
60. Chen, J. G., and Kempson, S. A. (1993) *Biochim. Biophys. Acta* **1149,** 299–304
61. Payne, J. A., Xu, J. C., Haas, M., Lytle, C. Y., Ward, D., and Forbush, B., III (1995) *J. Biol. Chem.* **270,** 17977–17985
62. Payne, J. A. (1997) *Am. J. Physiol.* **273,** C1516–C1525
63. Isenring, P., Jacoby, S. C., and Forbush, B., III (1998) *Proc. Natl. Acad. Sci. U. S. A.* **95,** 7179–7184
64. Reinstein, E., Scheffner, M., Oren, M., Ciechanover, A., and Schwartz, A. (2000) *Oncogene* **19,** 5944–5950
65. Cheng, J., Moyer, B. D., Milewski, M., Loffing, J., Ikeda, M., Mickle, J. E., Cutting, G. R., Li, M., Stanton, B. A., and Guggino, W. B. (2002) *J. Biol. Chem.* **277,** 3520–3529
66. Wang, S., Raab, R. W., Schatz, P. J., Guggino, W. B., and Li, M. (1998) *FEBS Lett.* **427,** 103–108
67. Wang, S., Yue, H., Derin, R. B., Guggino, W. B., and Li, M. (2000) *Cell* **103,** 169–179
68. Hernando, N., Deliot, N., Gisler, S. M., Lederer, E., Weinman, E. J., Biber, J., and Murer, H. (2002) *Proc. Natl. Acad. Sci. U. S. A.* **99,** 11957–11962
69. Plata, C., Meade, P., Hall, A., Welch, R. C., Vazquez, N., Hebert, S. C., and Gamba, G. (2001) *Am. J. Physiol.* **280,** F574–F582
70. Plata, C., Meade, P., Vazquez, N., Hebert, S. C., and Gamba, G. (2002) *J. Biol. Chem.* **277,** 11004–11012
71. Plata, C., Mount, D. B., Rubio, V., Hebert, S. C., and Gamba, G. (1999) *Am. J. Physiol.* **276,** F359–F366
72. Lopes, A. I., Almeida, A. G., Costa, A. E., Costa, A., and Leite, M. (1998) *Acta Med. Port* **11,** 1121–1125
73. Morris, R. C., Jr. (1968) *J. Clin. Investig.* **47,** 1389–1398
74. Salvatore, F., Izzo, P., and Paolella, G. (1986) *Horiz. Biochem. Biophys.* **8,** 611–665
75. Christova, T. Y., Orosz, F., and Ovadi, J. (1996) *Biochem. Biophys. Res. Commun.* **228,** 272–277
76. O'Reilly, G., and Clarke, F. (1993) *FEBS Lett.* **321,** 69–72
77. Meade, P., Hoover, R. S., Plata, C., Vazquez, N., Bobadilla, N. A., Gamba, G., and Hebert, S. C. (2003) *Am. J. Physiol.* **284,** F1145–F1154